REPORT DOCUMENTATION PAGE

Form Approved
OMB No. 0704-0188

1. REPORT DATE *(DD-MM-YYYY)*
09-05-2014

2. REPORT TYPE
Journal Article

3. DATES COVERED *(From - To)*

4. TITLE AND SUBTITLE
Issues for Storing Plant-based Alternative Fuels in Marine Environments

5a. CONTRACT NUMBER

5b. GRANT NUMBER

5c. PROGRAM ELEMENT NUMBER
0601153N

6. AUTHOR(S)
Jason S. Lee, Richard I. Ray, Brenda J. Little, Kathleen E. Duncan, Deniz F. Aktas, Athenia L. Oldham, Irene A. Davidova and Joseph M. Suflita

5d. PROJECT NUMBER

5e. TASK NUMBER

5f. WORK UNIT NUMBER
73-9611-02-5

7. PERFORMING ORGANIZATION NAME(S) AND ADDRESS(ES)
Naval Research Laboratory
Oceanography Division
Stennis Space Center, MS 39529-5004

8. PERFORMING ORGANIZATION REPORT NUMBER
NRL/JA/7330--12-1550

9. SPONSORING/MONITORING AGENCY NAME(S) AND ADDRESS(ES)
Office of Naval Research
One Liberty Center
875 North Randolph Street, Suite 1425
Arlington, VA 22203-1995

10. SPONSOR/MONITOR'S ACRONYM(S)
ONR

11. SPONSOR/MONITOR'S REPORT NUMBER(S)

12. DISTRIBUTION/AVAILABILITY STATEMENT
Approved for public release, distribution is unlimited.

13. SUPPLEMENTARY NOTES

14. ABSTRACT

Two coastal seawaters (Key West, FL, USA and the Persian Gulf, Bahrain, representing oligotrophic and eutrophic environments, respectively) were used to evaluate potential biodegradation and corrosion problems during exposure to alternative and conventional fuels. Uncoated carbon steel was exposed at the fuel/seawater interface and polarization resistance was monitored. Under typical marine storage conditions, dioxygen in natural seawater exposed to fuel and carbon steel was reduced to < 0.1 parts-per-million within 2 d due to consumption by corrosion reactions and aerobic microbial respiration. Sulfides, produced by anaerobic sulfate-reducing bacteria, and chlorides were co-located in corrosion products. Transient dioxygen influenced both metabolic degradation pathways and resulting metabolites. Catechols, indicative of aerobic biodegradation, persisted after 90 d exposures. Detection of catechols suggested that initial exposure to dioxygen resulted in the formation of aerobic metabolites that exacerbated subsequent corrosion processes.

15. SUBJECT TERMS
biodiesel, alternative fuel, seawater, corrosion, carbon steel

16. SECURITY CLASSIFICATION OF: a. REPORT	b. ABSTRACT	c. THIS PAGE	17. LIMITATION OF ABSTRACT	18. NUMBER OF PAGES	19a. NAME OF RESPONSIBLE PERSON
Unclassified	Unclassified	Unclassified	UU	9	Jason Lee

19b. TELEPHONE NUMBER *(Include area code)*
(228) 688-4494

Bioelectrochemistry 97 (2014) 145–153

Contents lists available at ScienceDirect

Bioelectrochemistry

journal homepage: www.elsevier.com/locate/bioelechem

Issues for storing plant-based alternative fuels in marine environments

Jason S. Lee [a,*], Richard I. Ray [a], Brenda J. Little [a], Kathleen E. Duncan [b], Deniz F. Aktas [b], Athenia L. Oldham [b], Irene A. Davidova [b], Joseph M. Suflita [b]

[a] *Naval Research Laboratory, 1009 Balch Blvd., Stennis Space Center, MS 39529, USA*
[b] *Department of Microbiology and Plant Biology, 770 Van Vleet Oval, University of Oklahoma, Norman, OK 73019, USA*

ARTICLE INFO

Article history:
Received 30 November 2012
Received in revised form 26 September 2013
Accepted 17 December 2013
Available online 24 December 2013

Keywords:
Biodiesel
Alternative fuel
Seawater
Corrosion
Carbon steel

ABSTRACT

Two coastal seawaters (Key West, FL, USA and the Persian Gulf, Bahrain, representing oligotrophic and eutrophic environments, respectively) were used to evaluate potential biodegradation and corrosion problems during exposure to alternative and conventional fuels. Uncoated carbon steel was exposed at the fuel/seawater interface and polarization resistance was monitored. Under typical marine storage conditions, dioxygen in natural seawater exposed to fuel and carbon steel was reduced to <0.1 parts-per-million within 2 d due to consumption by corrosion reactions and aerobic microbial respiration. Sulfides, produced by anaerobic sulfate-reducing bacteria, and chlorides were co-located in corrosion products. Transient dioxygen influenced both metabolic degradation pathways and resulting metabolites. Catechols, indicative of aerobic biodegradation, persisted after 90 d exposures. Detection of catechols suggested that initial exposure to dioxygen resulted in the formation of aerobic metabolites that exacerbated subsequent corrosion processes.

1. Introduction

Increasing energy costs and environmental concerns have underscored the need for sustainable renewable fuels. Major efforts in alternative fuel development have focused on pyrolysis of lignocellulosic biomass [1] and microbial (including microalgal) production of lipid-based fuels [2]. Algal biofuels are based on the high lipid content of the algal cell as a source for high energy density transportation fuels [3]. The feasibility of producing large quantities of fatty acid methyl ester (FAME) and lipid-based fuels has been demonstrated. An isoparaffin-rich jet fuel derived from camelina, a nonfood oilseed crop, was flight tested by a commercial airline [4]. Results indicated that the hydroprocessed renewable jet fuel (HRJ) met all engine and performance specifications with reduced environmental emission. In 2010, the US Navy successfully tested a blended 50% algae-based and 50% NATO F-76 fuel in riverine command boats (http://greenfleet.dodlive.mil/).

However, the real challenge for plant-based fuels is not production capacity or combustion characteristics in an engine. Plant-derived alternative fuels must remain stable under storage and use conditions. Fuel degradation can take place in the fuel supply chain and in the vehicle fuel system and the products of biodegradation may be corrosive. Speidel et al. [5] concluded that fuels having a higher degree of components derived from renewable sources had a higher degradability potential than those composed of petroleum components. Blin et al. [1] measured the biodegradability of biomass pyrolysis oils and discussed the biodegradability of other fuels. Biomass pyrolysis oils had biodegradabilities of 41–50% after 28 d. Linear aliphatic alkanes of Fischer-Tropsch diesel were biodegraded at a similar rate. Vegetables oils were degraded less than their modified methyl esters. FAME fuels had biodegradabilities greater than 87%. The authors concluded that branching and aromatic compounds make fossil fuels more stable and less biodegradable.

Fuels are often stored for months in steel tanks and exposed to varying amounts of fresh water and dioxygen. Fuels can also come in direct contact with marine waters in ships equipped with seawater-compensated ballast tanks. In these systems, seawater is used to compensate for volume and weight loss as fuel is consumed. Corrosion associated with storing fuels in steel in contact with natural seawater is expected to be related to seawater chemistry/microbiology, fuel chemistry/microbiology and dioxygen. A series of experiments were designed to address the following specific questions related to fuel biodegradation and corrosion: Are issues for storing alternative fuels in contact with natural seawater different from those experienced with petroleum-based fuels? Does initial dioxygen concentration in the seawater and fuel phases affect biodegradation? Do differences in seawater compositions (chemical and microbiological) influence degradation of alternative fuels and the resulting corrosion? Data from those experiments are presented herein to more generally discuss issues related to the storage of alternative fuels.

2. Materials and methods

2.1. Seawater

Coastal seawaters were collected from Key West, FL, USA and in the Persian Gulf at Mina Sulman, Bahrain and used as inocula and growth

---

* Corresponding author.
E-mail address: jason.lee@nrlssc.navy.mil (J.S. Lee).

1567-5394/$ – see front matter. Published by Elsevier B.V.
http://dx.doi.org/10.1016/j.bioelechem.2013.12.003

20150917421

media, as previously described [6]. Initial Key West seawater (KW) and Persian Gulf seawater (PG) chemistries are presented in Table 1.

2.2. Fuels

Three neat fuels were used in these experiments including soy-derived fatty acid methyl ester biodiesel (B100), U.S. military specified petroleum diesel (F-76) and petroleum jet propellant (JP-5). In addition, two hydroprocessed fuels, algae-derived F-76 (HRD-76) and camelina-derived JP-5 (HRJ-5) were blended in a 50/50 volume percent ratio (v/v) with their petroleum counterparts to produce alternative fuels 50/50 F-76/HRD-76 and 50/50 JP-5/HRJ-5.

2.3. Metal coupons

Carbon steel (CS) (UNS C10200) coupons (0.20% C, 0.47% Mn, 0.012% P, 0.013% Si, bal. Fe) (1.58 cm dia. × 0.16 cm) were individually mounted in epoxy (Epothin™, Buehler Ltd., Lake Bluff, IL) that established an exposed area of 2 cm^2. Prior to mounting, an insulated wire was attached to the backside of each coupon with conductive epoxy and carbon tape to achieve electrical connection. The as-received mill scale finish was left intact. Prior to exposure, mounted coupons (electrodes) were rinsed sequentially with acetone, ethanol and dried with N_2.

2.4. Exposure chambers

Chambers were constructed to contain seawater and fuel combinations or unamended seawater. The chambers were rectangular (19 cm width, 31 cm length and 31 cm height) and constructed from heavy gauge, chemical resistant, opaque black plastic. Combinations of seawater (4.5 L) with or without fuel addition (3 L) were sealed in the plastic chambers as previously described [7,8]. Exposures without fuel contained 7.5 L of seawater.

Schematic representation of the exposure chamber is shown in Fig. 1. Triplicate electrodes were arranged with exposed CS surfaces orientated vertically within the chambers at the fuel/seawater interface, where the lighter fuel formed a separate layer on top of the seawater. If no fuel was present, coupons were fully immersed in seawater. Polarization resistance (R_p) (Ω cm^2) of the exposed coupon area (2 cm^2) was monitored daily using the linear polarization technique [9] in accordance with ASTM Standard G5-94 [10]. The inverse of polarization resistance (R_p^{-1}) (Ω^{-1} cm^{-2}) is proportional to the instantaneous corrosion rate [10]. Silver/silver chloride (Ag/AgCl) electrodes and platinum/niobium (Pt/Nb) mesh were used as reference and counter electrodes, respectively. CS surfaces were oriented towards the counter and reference electrodes. An Oxyguard® (Point Four Systems, Coquitlam, BC, Canada) dioxygen probe was placed at the bottom of each chamber and monitored daily. Dioxygen concentration was measured in units of parts-per-million (ppm).

2.5. Exposure conditions

Chambers were either left open to air (aerobic) via a small port or were placed in an anaerobic glove box (0.01 v/v CO_2, 10 v/v H_2, bal. N_2) to maintain a seawater pH of 7.8–8.2 [6]. All experiments were carried out at room temperature (22 ± 1 °C). Exposures were performed in three separate experimental phases as listed in Table 2. Phases I and III lasted 90 d while Phase II lasted 60 d. Phase I had seawater-only exposures, Phase II included a B100 addition to seawater while Phase III examined military fuel additions.

Table 1
Initial chemistries of Key West (KW) and Persian Gulf (PG) seawaters.

Seawater	pH	$C(salt)^a/g\ kg^{-1}$	$C(C_{org})^b/mg\ L^{-1}$	$C(SO_4^{2-})/mg\ L^{-1}$
KW	7.82	38	1.79	3864
PG	7.98	44	1.94	4696

[a] Salinity of seawater in grams of salt per kilogram of solution.
[b] Concentration of total organic carbon.

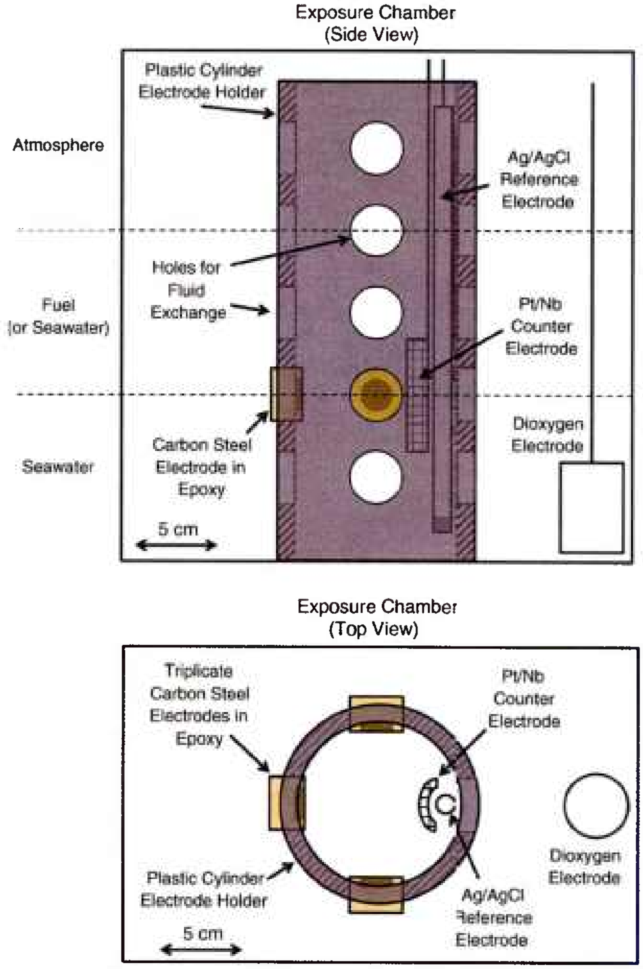

Fig. 1. Schematic of the fuel/seawater exposure chamber. Epoxy embedded carbon steel electrodes were held in a vertical orientation by a plastic cylinder with holes cut for electrode mounting and fluid exchange. Triplicate electrodes were exposed at the fuel/seawater interface or fully immersed in seawater. Reference (Ag/AgCl) and counter (Pt/Nb) electrodes provided the ability to monitor electrochemical parameters of each carbon steel electrode individually. A dioxygen electrode was placed at the bottom of the exposure chamber for transient dioxygen measurement.

Table 2
Experimental matrix.

Exposure condition	Seawater	Fuel	Atmosphere
Phase I	KW	–	Aerobic
Different seawaters without	PG	–	Aerobic
fuel addition	KW	–	Anaerobic
	PG	–	Anaerobic
Phase II	KW	B100	Aerobic
Different seawaters with identical	KW	B100	Anaerobic
fuel addition	PG	B100	Anaerobic
Phase III	KW	F-76	Anaerobic
One seawater with different	KW	50/50 F-76/HRD-76	Anaerobic
fuel additions	KW	JP-5	Anaerobic
	KW	50/50 JP-5/HRJ-5	Anaerobic

KW = Key West, FL, USA seawater; PG = Persian Gulf seawater.

2.6. Post-exposure analysis

For Phase III only, dissolved H_2S concentration in the seawaters was measured at the conclusion of the exposure period following procedures described previously [6]. CS coupons removed from the epoxy and acid cleaned for 10 min in 1:1 HCl acid (sp gr 1.19):deionized water (6.03 M) with 3.5 g L^{-1} (24.8 mM) hexamethylene tetramine [11] at room temperature. CS coupons were imaged (before and after acid cleaning) in an environmental scanning electron microscope (ESEM) at an accelerating voltage of 20 keV. Energy dispersive spectroscopy (EDS) was used to evaluate the elemental weight % (w/w) chemical composition of corrosion products. Phase III coupons were scanned using a Nanovea (Irvine, CA) Model PS50 non-contact optical profiler with a 3.5 mm optical pen to reconstruct high contrast 3-D digital images.

2.7. Metabolite profiling

Phase III military fuel/seawater combinations were examined for polar metabolites and other components that partitioned into the seawater. Baseline measurements were performed where fuels were mixed with equal volumes of seawater (KW), stirred overnight, and the resulting aqueous phase was acidified (10 M HCl; pH $\leq$ 2) prior to an ethyl acetate extraction. Extracts were concentrated, derivatized and analyzed by gas chromatography–mass spectrometry (GC–MS) as previously described [12]. This baseline was compared to the fuel–seawater mixtures that were incubated for 90 d and analyzed in an identical manner. Identifications were made by comparison of the GC retention times and MS fragmentation patterns with commercial standards (Sigma-Aldrich, St Louis, MO) that were similarly analyzed, or by comparison with the NIST Mass Spectral Library, Version 2.0a.

3. Results

3.1. Dioxygen

For all experiments, dioxygen in KW and PG was initially 8 ppm (250 μM). The transient nature of dioxygen concentration was independent of seawater origin (KW vs. PG), but was a function of exposure conditions. For aerobic exposures with and without fuel, dioxygen concentration decreased to 4 ppm (125 μM) after 4 d and to ~2 ppm (60 μM) after 10 d (Fig. 2). Over the remainder of the exposure, dioxygen concentration fluctuated between 2 and 4 ppm. For seawaters surrounded by an anaerobic atmosphere, dioxygen concentration was depleted to detection limits of the probe (0.1 ppm ≅ 3 μM) within 2 d with or without fuel addition.

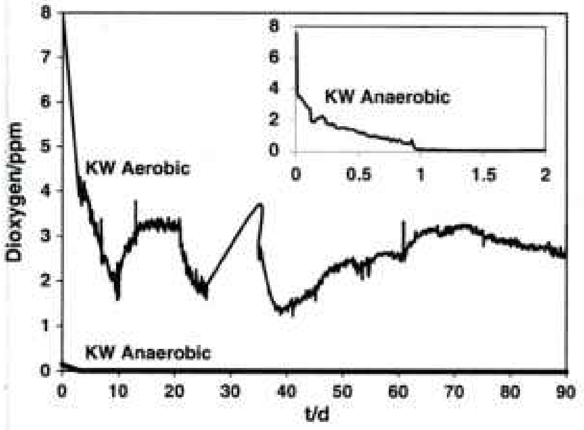

Fig. 2. Transient dioxygen profiles. Dioxygen profiles (parts-per-million [ppm]) of Key West seawater (KW) without fuel addition during exposure with carbon steel in aerobic and anaerobic gas environments. The inset is a magnified view of the early anaerobic exposure. These profiles are also representative of seawater exposures with fuel addition. [18]

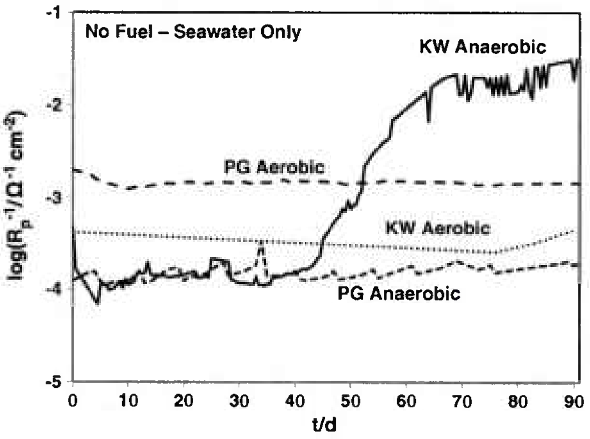

Fig. 3. Carbon steel R_p^{-1} trends in seawaters without fuel addition. Averaged logarithmic R_p^{-1} (Ω^{-1} cm^{-2}) of carbon steel in seawaters (without fuel addition) as a function of exposure time (d). PG = Persian Gulf seawater, KW = Key West seawater, Aerobic = open to air, Anaerobic = inside anaerobic glove box with gas mixture of 0.01 v/v CO_2, 10 v/v H_2 and bal. N_2.

3.2. Phase I. Different seawaters (KW & PG) without fuel addition

Fig. 3 shows average R_p^{-1} (Ω^{-1} cm^{-2}) as a function of the 90 d exposure period for CS exposed to KW and PG with aerobic and anaerobic atmospheres in the absence of fuel. CS in aerobic PG exhibited lower R_p^{-1} (1.5×10^{-3} Ω^{-1} cm^{-2}) than CS in aerobic KW ($R_p^{-1} = 3 \times 10^{-4}$ Ω^{-1} cm^{-2}). The anaerobic PG condition resulted in the lowest overall CS R_p^{-1} (1.5×10^{-4} Ω^{-1} cm^{-2}). CS R_p^{-1} in KW with anaerobic atmosphere was identical to the PG exposures until d 45 where R_p^{-1} (CS in KW) increased and by d 70 had reached 2×10^{-2} Ω^{-1} cm^{-2}. Both anaerobic KW and PG exposures had distinct sulfide odors after 90 d with KW producing a much stronger smell. KW and PG aerobic exposures did not produce a sulfide odor. CS surfaces exposed to aerobic conditions were covered by voluminous red-orange corrosion products. Corrosion products were composed mainly of Fe with lesser amounts of Cl and S (Table 3). Exposure to aerobic PG resulted in significantly higher concentrations of Cl (8.0 ± 0.3 w/w) compared to KW exposure (1.4 ± 1.0 w/w). Anaerobic conditions resulted in black corrosion products that contained significant amounts of S in addition to Fe and Cl. CS exposed to anaerobic KW had the highest amount of S (15.4 ± 3.0 w/w) compared to CS exposed to anaerobic PG (1.4 ± 0.7 w/w).

After acid cleaning, coupons were reexamined in the ESEM. For aerobic KW and PG exposures, corrosion morphology was uniformly

Table 3
Corrosion product chemistry via energy dispersive spectroscopy (EDS).[a]

	Seawater	Fuel	Atmosphere	C(S)[b]/w/w	C(Cl)[c]/w/w
Phase I	KW		Aerobic	0.4 ± 0.2	1.4 ± 1.0
	PG		Aerobic	0.8 ± 0.3	8.0 ± 0.3
	KW		Anaerobic	15.4 ± 3.0	1.2 ± 0.8
	PG		Anaerobic	1.4 ± 0.7	0.9 ± 0.1
Phase II	KW	B100	Aerobic	1.0 ± 0.4	7.7 ± 3.9
	KW	B100	Anaerobic	26.9 ± 5.8	4.9 ± 1.7
	PG	B100	Anaerobic	1.4 ± 0.4	4.0 ± 3.0
Phase III	KW	JP-5	Anaerobic	20.1 ± 2.2	1.6 ± 0.4
	KW	JP-5/HRJ-5 50/50	Anaerobic	6.1 ± 0.6	0.2 ± 0.2
	KW	F-76	Anaerobic	20.4 ± 4.0	0.4 ± 0.3
	KW	F-76/HRD-76 50/50	Anaerobic	9.4 ± 2.4	1.5 ± 1.2

[a] EDS provides only elemental composition in weight % (w/w), no valence state information.

[b] Assumed to be sulfate/sulfide for aerobic/anaerobic exposures respectively.

[c] Assumed to be chloride.

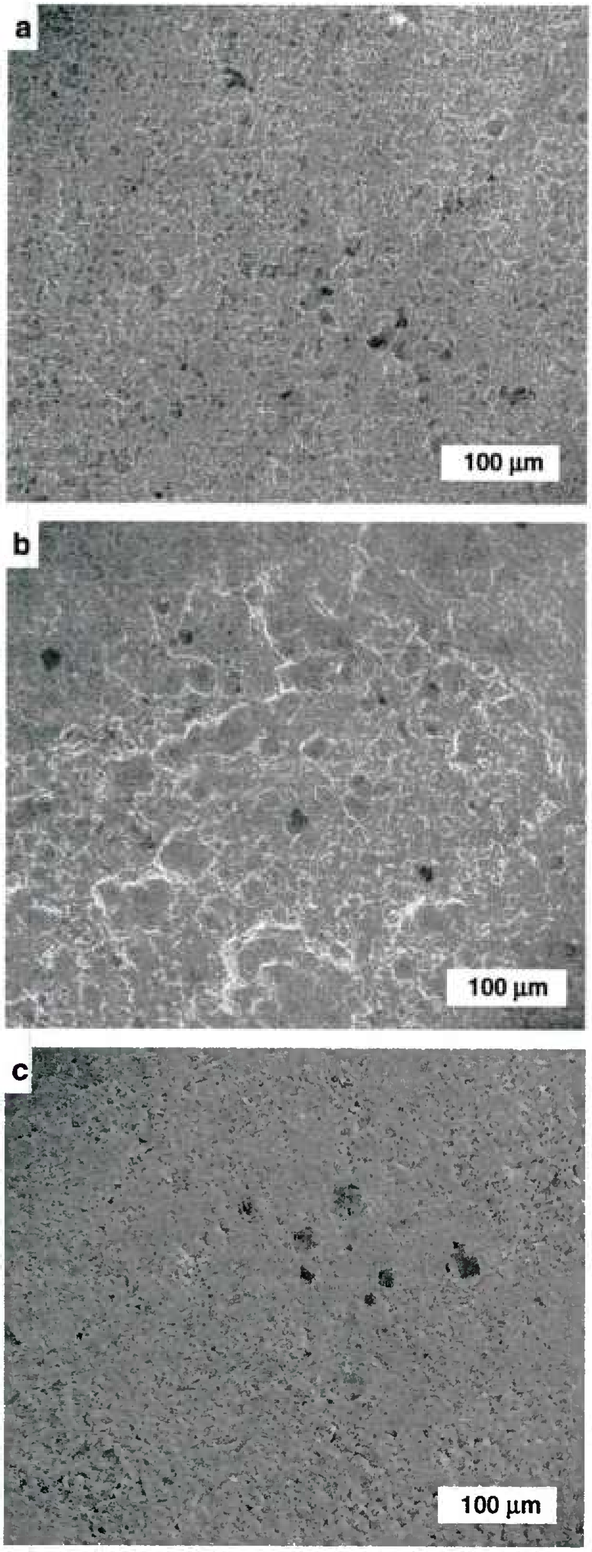

Fig. 4. Carbon steel corrosion morphology after exposure to seawaters. Representative carbon steel (acid cleaned) corrosion morphology after 90 d exposure to a) aerobic KW, b) anaerobic KW and c) anaerobic PG. PG = Persian Gulf seawater, KW = Key West seawater, Aerobic = open to air, Anaerobic = inside anaerobic glove box with gas mixture of 0.01 v/v CO_2, 10 v/v H_2 and bal. N_2.

exhibiting both crystallographic and granular attacks in addition to a few small 10 µm pits (Fig. 4a). In comparison, CS exposure to anaerobic KW resulted in larger pits (100 µm) in addition to the 10 µm pits (Fig. 4b). CS exposed to anaerobic PG exhibited isolated pitting surrounded by lightly etched metal (Fig. 4c). Pits in CS from anaerobic PG exposure were intermediate in size (40 µm) to the aerobic exposures and the anaerobic KW exposure. The highest density of pits was for CS exposed to anaerobic KW.

3.3. Phase II. Different seawaters (PG & KW) with identical fuel addition (B100)

Fig. 5 shows average R_p^{-1} (Ω^{-1} cm^{-2}) as a function of the 60 d exposure period for CS exposed at the fuel/seawater interfaces of aerobic (KW) and anaerobic (KW & PG) amended with B100. Initially, CS exposed to anaerobic KW with B100 resulted in R_p^{-1} that decreased from 3×10^{-4} to 1×10^{-6} Ω^{-1} cm^{-2} but at d 12 a sulfide odor was detected followed by increased R_p^{-1} to 1×10^{-3} Ω^{-1} cm^{-2} by d 23. CS exposed to KW with B100 under aerobic atmosphere resulted in $R_p^{-1} = 1 \times 10^{-4}$ Ω^{-1} cm^{-2} over the first 50 d. CS R_p^{-1} then dropped (1.5×10^{-5} Ω^{-1} cm^{-2}), and remained constant for the last 10 d. PG with B100 under anaerobic conditions produced relatively lower CS R_p^{-1} (<10^{-6} Ω^{-1} cm^{-2} average). Similar to Phase I results, after 60 d the anaerobic KW exposure had a very strong putrid, sulfide smell while the odor was less pronounced in the anaerobic PG exposure. Also, no sulfide odor was detected from the aerobic KW exposure. A buildup of cloudy oily residue across CS surfaces coincided with the fuel/seawater interfaces for all exposure conditions. Exposure to aerobic KW with B100 resulted in red–orange corrosion products covering the CS surface below the B100/KW interface (Fig. 6(a)). A dark corrosion product (not shown) was beneath the outer red–orange layer, but only below the fuel/seawater interface. CS surfaces after exposure to anaerobic KW and B100 were completely covered by black corrosion products (Fig. 6(b)). The anaerobic exposure into PG and B100 resulted in black corrosion products on the CS surface at and below the B100/PG interface (Fig. 6(c)). Similar to Phase I experiments, black anaerobic corrosion products contained significant amounts of S in addition to Fe and Cl (Table 3). Anaerobic KW exposure resulted in CS corrosion products with the highest amount of S (26.9 ± 5.8 w/w) compared to CS surfaces exposed to anaerobic PG (1.4 ± 0.4 w/w). Aerobic KW exposure resulted in corrosion products low in S (1.0 ± 0.4 w/w) but high in Cl (7.7 ± 3.9 w/w). Both anaerobic exposures resulted in lower Cl

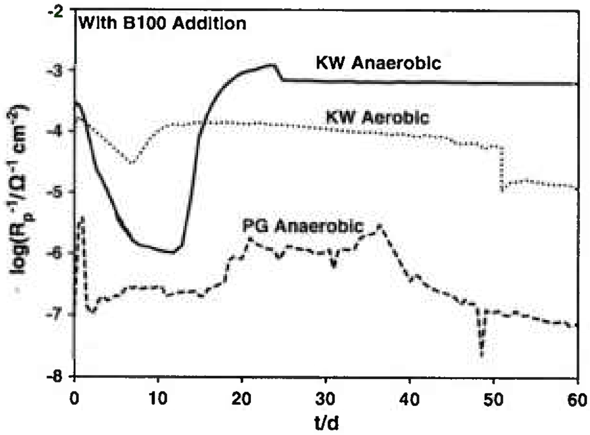

Fig. 5. Carbon steel R_p^{-1} trends in seawaters with B100 addition. Averaged logarithmic R_p^{-1} (Ω^{-1} cm^{-2}) of carbon steel at the seawater/B100 interface as a function of exposure time (d). PG = Persian Gulf seawater, KW = Key West seawater, Aerobic = open to air, Anaerobic = inside anaerobic glove box with gas mixture of 0.01 v/v CO_2, 10 v/v H_2 and bal. N_2.
Modified from Lee et al. [19].

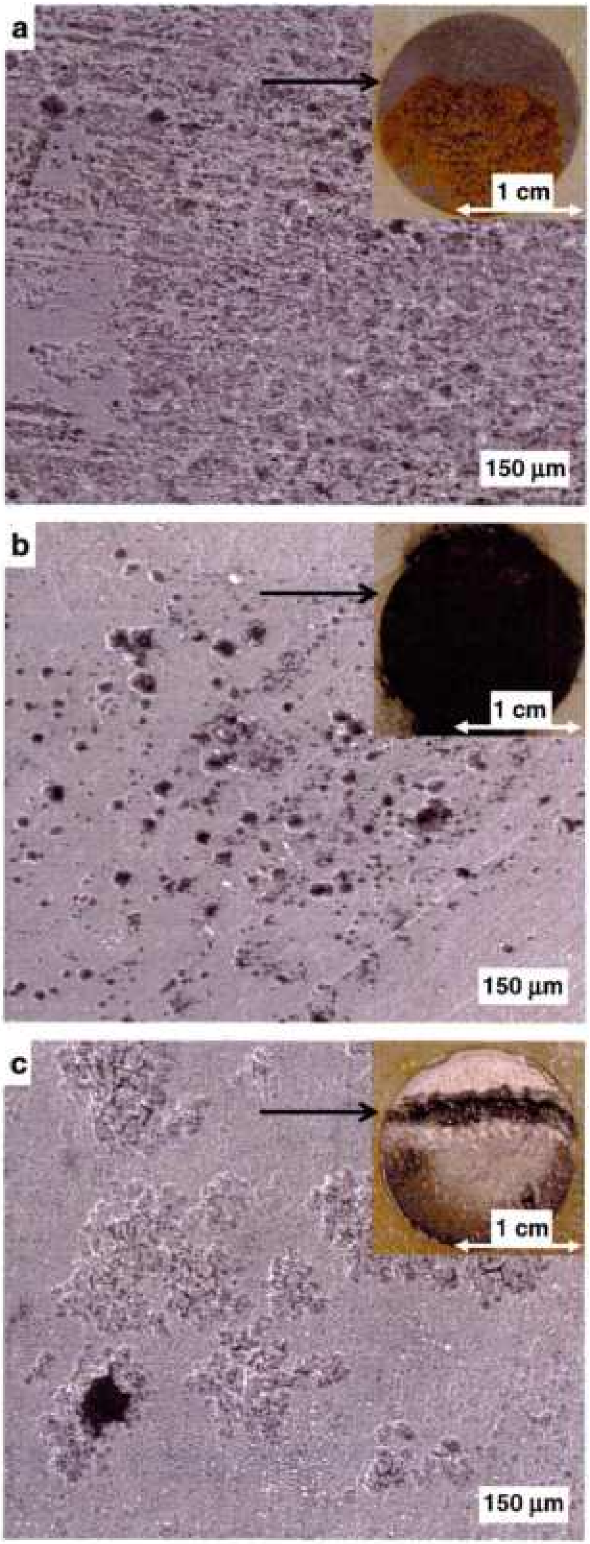

Fig. 6. Carbon steel corrosion morphology after exposure to seawaters with B100 addition. Representative carbon steel (acid cleaned) corrosion morphology after 60 d exposure to B100 with a) aerobic KW, b) anaerobic KW and c) anaerobic PG. Insets show carbon steel coupon at the time of removal (prior to acid cleaning) illustrating the fuel/seawater interfaces (arrows). PG = Persian Gulf seawater, KW = Key West seawater, Aerobic = open to air, Anaerobic = inside anaerobic glove box with gas mixture of 0.01 v/v CO_2, 10 v/v H_2 and bal. N_2.

amounts in the corrosion products, 4.9 ± 1.7 w/w and 4.0 ± 3.0 w/w for KW and PG, respectively.

After acid cleaning, coupons were reexamined in the ESEM. Corrosion morphology was uniform after aerobic KW exposure with B100 (Fig. 6). Anaerobic exposures with B100 resulted in isolated pitting in the CS. Pits were not necessarily associated with the fuel/seawater interface. Exposure to anaerobic KW with B100 resulted in more pits but the pits were smaller (50 µm dia.) and less deep (25 µm) than those from the PG exposure (100 µm dia., 80 µm depth).

3.4. Phase III. A single seawater (KW) with different fuel additions (military fuels)

Fig. 7 shows average R_p^{-1} trends of CS exposed in anaerobic KW with additions of JP-5 fuels. At the experimental onset, R_p^{-1} for both exposures was $2 \times 10^{-4}\ \Omega^{-1}\ cm^{-2}$. Over the first 10–12 d, CS R_p^{-1} decreased by an order-of-magnitude (or less), with the greater decrease for the exposure with JP-5. R_p^{-1} for CS exposed in JP-5 reached a maximum by d 30 ($1 \times 10^{-2}\ \Omega^{-1}\ cm^{-2}$) and remained near that magnitude for the remainder of the exposure. CS exposed in 50/50 JP-5/HRJ-5 had R_p^{-1} an order-of-magnitude lower ($1 \times 10^{-3}\ \Omega^{-1}\ cm^{-2}$) at d 30 and increased to $4 \times 10^{-3}\ \Omega^{-1}\ cm^{-2}$ by d 90. R_p^{-1} trends for CS immersed in anaerobic KW with F-76 and 50/50 F-76/HRD-76 additions are shown in Fig. 8. Over the first 7 d, CS R_p^{-1} decreased by an order-of-magnitude from $2 \times 10^{-4}\ \Omega^{-1}\ cm^{-2}$ to $2 \times 10^{-5}\ \Omega^{-1}\ cm^{-2}$. On d 10, R_p^{-1} increased. By d 30, R_p^{-1} had increased by two orders-of-magnitude compared with the minimum d 7 value. For the remainder of the 90 d exposure, R_p^{-1} remained at the elevated level.

At the 90 d conclusion, all exposures had a "rotten egg" sulfide smell. Dark corrosion products were observed on all CS coupons exposed at the fuel/seawater interfaces. Corrosion products in both the water and fuel phases contained significant amounts of S, with Cl concentrations of ~1 w/w for all exposures (Table 3). The highest S concentrations (~20 w/w) were with additions of F-76 and JP-5. The lowest S concentration was associated with 50/50 JP-5/HRJ-5 (6.1 ± 0.6 w/w). Dissolved sulfide was detected in all seawaters. The highest concentration (4.69 mM) was observed in the seawater with 50/50 JP-5/HRJ-5 fuel incubations.

After acid cleaning, coupons were reexamined in the ESEM. For JP-5 and 50/50 JP-5/HRJ-5 exposures, the entire CS surfaces exhibited general attack with a few small isolated pits (50 mm dia., 50 mm depth) (Fig. 9(a), (c)). Localized regions of unattacked metal (original mill finish represented as gray areas in Fig. 9(a–d)) were observed

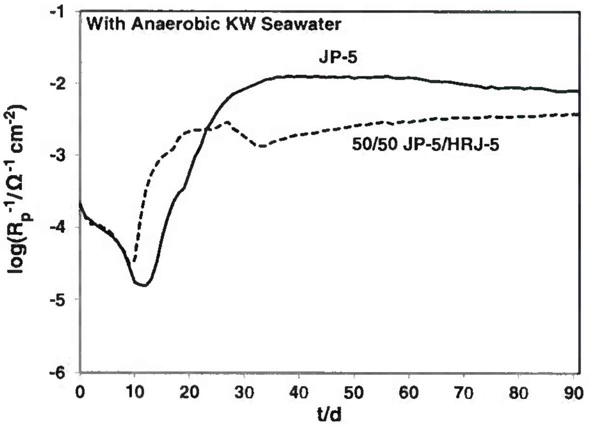

Fig. 7. Carbon steel R_p^{-1} trends in anaerobic seawater and jet fuels. Averaged logarithmic R_p^{-1} ($\Omega^{-1}\ cm^{-2}$) of carbon steel at the seawater/fuel interface as a function of exposure time (d). KW = Key West, JP-5 = petroleum JP-5 fuel, 50/50 JP-5/HRJ-5 = 50/50 blend of petroleum JP-5 and hydroprocessed camelina-derived alternative JP-5 fuel (HRJ-5). Anaerobic = inside anaerobic glove box with gas mixture of 0.01 v/v CO_2, 10 v/v H_2 and bal. N_2.

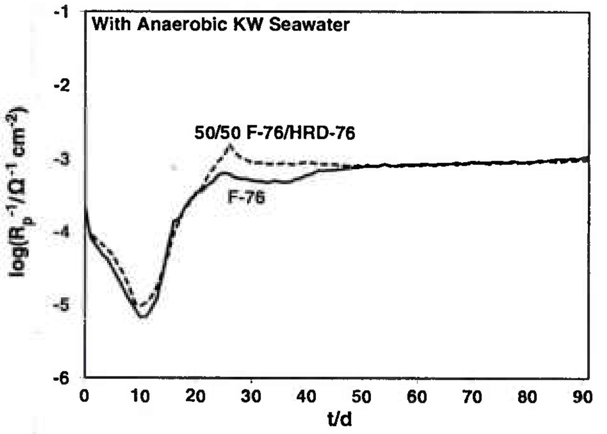

Fig. 8. Carbon steel R_p^{-1} trends in anaerobic seawater and jet fuels. Averaged logarithmic R_p^{-1} (Ω^{-1} cm^{-2}) of carbon steel at the seawater/fuel interface as a function of exposure time (d). KW = Key West, F-76 = petroleum F-76 fuel, 50/50 F-76/HRD-76 = 50/50 blend of petroleum F-76 and hydroprocessed algae-derived alternative F-76 fuel (HRD-76). Anaerobic = inside anaerobic glove box with gas mixture of 0.01 v/v CO_2, 10 v/v H_2 and bal. N_2.

above and below the fuel/seawater interfaces. In comparison, F-76 and 50/50 F-76/HRD-76 exposures exhibited larger pits below the interface surrounded by unattacked metal (Fig. 9(b), (d)). Pits were wider and deeper in F-76 exposure (1000 μm dia., 100 μm deep) compared with 50/50 F-76/HRD-76 (700 μm dia., 70 μm deep). In general, more mill finish was retained (i.e. less surface was attacked) on CS exposed to KW and F-76 compared to the JP-5 fuel exposures.

Initially, all fuels (not including B100) and blends contained straight chain *n*-alkanes (C_{10} to C_{15}) that partitioned to the seawater phase (Figs. 10 & 11). *n*-Alkanes up to C_{23} from F-76 and 50/50 F-76/HRD-76 additions were detected (Fig. 11). A comparison of the chromatographic profiles before (initial) and after (final) the 90 d exposure indicated that all *n*-alkanes [C_{10} to C_{15}] in JP-5 were removed (Fig. 10, stars indicate loss of a particular *n*-alkane). The same pattern of *n*-alkane removal was observed for the 50/50 JP-5/HRJ-5. Moreover, several new peaks (not detected in either the original fuels or seawater) that corresponded to carbon chain lengths greater than C_{15}, were observed in all JP-5-related GC spectra after incubation.

A different pattern of hydrocarbon loss was evident with the F-76 fuels (Fig. 11). Removal of *n*-alkanes was far less prominent in the petro-F-76 incubations compared to the 50/50 F-76/HRD-76 exposures. When 50/50 F-76/HRD-76 was incubated with seawater, the preferential removal of *n*-alkanes (C_{10}–C_{23}) was apparent (Fig. 11, stars indicate loss of a particular *n*-alkane). Ratios of the integrated peak areas changed in the chromatographic profiles for lower (and not the higher) molecular weight *n*-alkanes, suggesting that simple dilution cannot account for the removal of these fuel components.

Qualitatively, a complex suite of branched alkanes (peaks intermediate to the *n*-alkane peaks) of varying carbon chain lengths (C_{10} to C_{19}) also partitioned to seawater from all fuel types. Longer chain branched alkanes were more pronounced in F-76 fuels (Fig. 11) than in JP-5

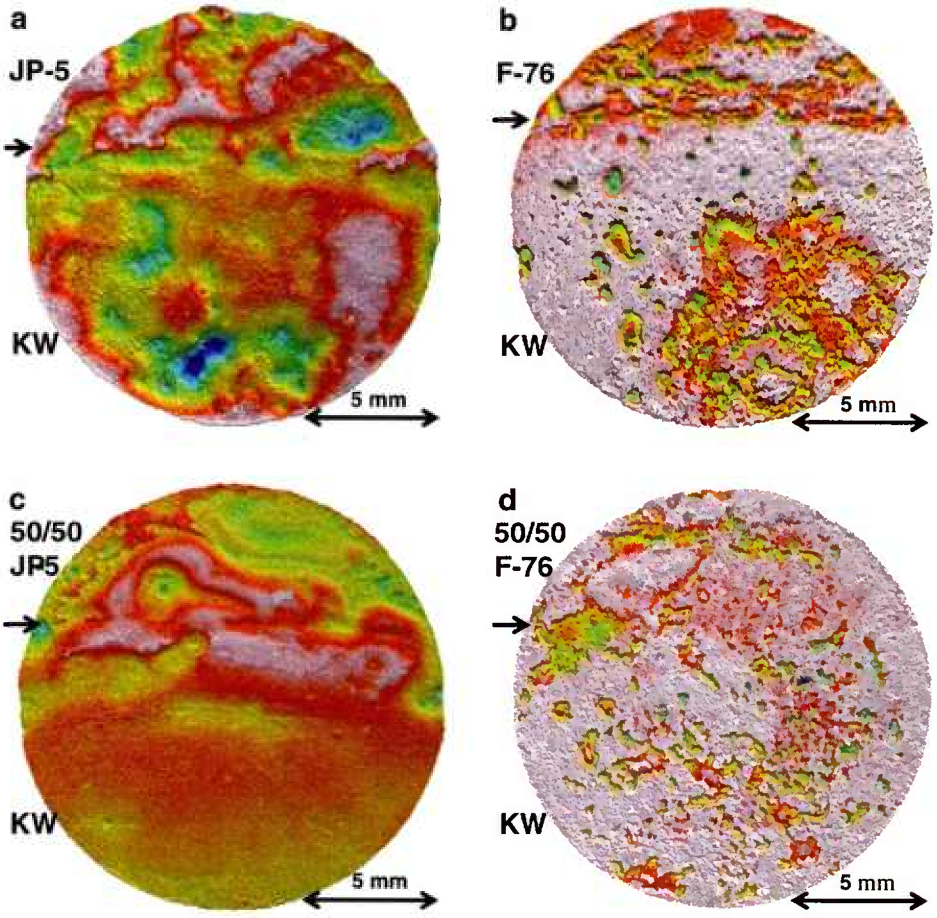

Fig. 9. Carbon Steel corrosion morphology after exposure to seawaters with military fuel addition. Representative 3-dimensional profilometry reconstructions of carbon steel (acid cleaned) corrosion morphology after 90 d exposure to anaerobic Key West seawater with a) JP-5 addition, b) F-76, c) 50/50 JP-5/HRJ-5 and d) 50/50 F-76/HRD-76. Black arrows indicate the position of the fuel/seawater interface. Gray color indicates original carbon steel surface with blue indicative of the deepest penetrations (100 μm). Anaerobic = inside anaerobic glove box with gas mixture of 0.01 v/v CO_2, 10 v/v H_2 and bal. N_2.

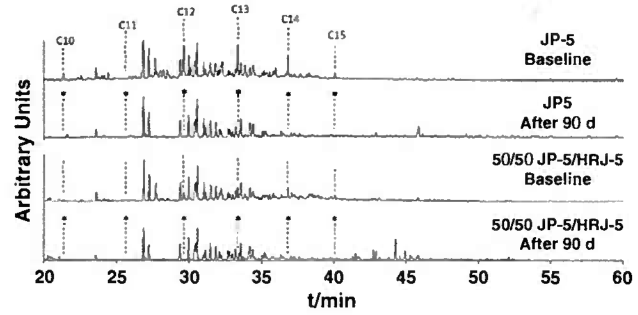

Fig. 10. Jet propellant fuel components in aqueous phase before and after incubation. Gas chromatographic retention time (t/min) profiles of the fuel components that partitioned into the aqueous phase (Key West seawater) after 1 and 90 d incubations. KW was exposed to petroleum (JP-5) and 50/50 blend of JP-5 and HRJ-5 (hydroprocessed camelina-derived JP-5) (50/50 JP-5/HRJ-5). Baseline profiles were generated after mixing of fuel/seawater for 1 d. The alkanes are labeled with their corresponding carbon chain lengths. The specific peaks are marked with dashed lines to make the comparison between profiles of different fuels easier. Stars indicate loss of a particular n-alkane. Y-axes are in arbitrary units with no quantitative analysis of relative concentrations.
Modified from Aktas et al. [20].

fuels (Fig. 10). Branched alkanes were almost completely depleted in the seawaters exposed to JP-5, 50/50 JP-5/HRJ-5 and 50/50 F-76/HRD-76, whereas they were only partially depleted in F-76.

No metabolites indicative of aerobic or anaerobic biodegradation of hydrocarbons were detected in fuel layers by GC–MS prior to incubation. At the end of the incubation, several putative metabolites were detected in all incubations. All incubations except those amended with F-76, contained catechol and/or a variety of alkylated catechols. Phenol, cresol and benzoate were other common metabolites in the incubations that could be formed under both aerobic and anaerobic conditions.

4. Discussion

Two coastal seawaters representing two different microbial and chemical environments were selected for the sulfide production and corrosion studies. KW is typical of open-ocean oligotrophic water. In the Persian Gulf, the total evaporation exceeds fresh water input, resulting in the concentration of dissolved species relative to those characteristic of typical seawater. Under aerobic conditions, PG produced higher R_p^{-1} values (higher proportional instantaneous corrosion rates) for CS than aerobic KW, as one would predict from the initial chemistries, i.e. higher salinity (Table 1, Fig. 3). However, under aerobic conditions (dioxygen <0.1 ppm), the observations were reversed, i.e. KW produced higher R_p^{-1} than PG. Lee et al. [6] compared the chemistry and microflora of the two natural coastal seawaters (KW & PG) maintained under anaerobic conditions. They demonstrated that despite higher levels of initial sulfate and total organic carbon in PG, orders of magnitude higher dissolved sulfide concentrations were measured in KW samples (e.g., 100 ppm vs. 0.01 ppm).

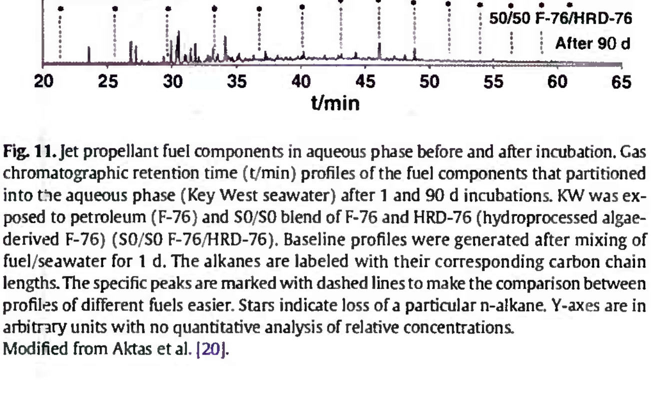

Fig. 11. Jet propellant fuel components in aqueous phase before and after incubation. Gas chromatographic retention time (t/min) profiles of the fuel components that partitioned into the aqueous phase (Key West seawater) after 1 and 90 d incubations. KW was exposed to petroleum (F-76) and 50/50 blend of F-76 and HRD-76 (hydroprocessed algae-derived F-76) (50/50 F-76/HRD-76). Baseline profiles were generated after mixing of fuel/seawater for 1 d. The alkanes are labeled with their corresponding carbon chain lengths. The specific peaks are marked with dashed lines to make the comparison between profiles of different fuels easier. Stars indicate loss of a particular n-alkane. Y-axes are in arbitrary units with no quantitative analysis of relative concentrations.
Modified from Aktas et al. [20].

The same trends, i.e., higher CS R_p^{-1} for anaerobic KW compared to anaerobic PG were observed when readily biodegradable [12] B100 was added. The presence of B100 caused an initial decrease in CS R_p^{-1} for all exposure conditions (Fig. 5). Lee et al. [13] demonstrated that B100 in contact with aerobic distilled water (simulating water of condensation) supported the growth of both bacteria and fungi in the water phase. However, the authors noted that CS corrosion was not observed after exposure to B100/water medium for 0.5 y. The authors suggested that B100 partitioned into the distilled water and was adsorbed onto the carbon steel surface causing sustained passivation. Electrochemical measurements confirmed passivity in the presence of B100.

The electrochemical behavior (Figs. 5, 7 and 8) of CS exposed to fuel/seawater combinations has been described previously [12]. The repeatability of the transient electrochemical curve independent of fuel type is consistent with an incubation period where dioxygen is consumed by corrosion reactions and microbial respiration (Fig. 2) and fuel components partition into the seawater resulting in CS passivation. The following hypothesis has been developed. After about 7 d, the activity of sulfate reducing bacteria (SRB) increased using dissolved fuel components or initial metabolites as carbon sources (electron donors) and sulfates as an electron acceptor to produce sulfides. As sulfide production increased over the next two weeks, R_p^{-1} increased by orders-of-magnitude until a steady state was reached where it remained elevated and stable. In fuel-unamended seawater, the lower measured sulfide levels and longer incubation period (45 d) prior to the onset of substantive corrosion, confirmed that fuel addition stimulated sulfide production and corrosion. Aktas et al. [12] reached the same conclusion in their study of soy-based biodiesel decomposition in seawater incubations.

Analysis of fuel constituents that partitioned to seawater suggested that many of the fuel components were biodegraded (Figs. 10 and 11). Nucleotide sequences coding for alkane monooxygenase, an enzyme which initiates aerobic alkane degradation, were obtained from all the fuel incubations except that with HRJ-5 [3], which supports the interpretation that alkane-degrading microbes were present in the fuel incubations. Removal of almost all alkanes from the incubations of bio-based fuels (and their 50/50 blends) suggested that these fuels were somewhat more amenable to decay than their petroleum-based fuel counterparts. However, JP-5 was an exception in this regard since all *n*-alkane peaks were removed.

At the end of 90 d a variety of putative metabolites were observed in the incubations supporting the contention that hydrocarbon removal was due at least in part to biodegradation by seawater microorganisms. Benzoate, cresols and alkanoic acids observed in the incubations could conceivably be the result of either aerobic or anaerobic metabolic processes. However, the formation of a series of catechols was particularly diagnostic. The appearance of catechols could only result from aerobic biodegradation of aromatic compounds [14]. Aerobic microorganisms capable of catechol metabolism typically elaborate dioxygenases that require dioxygen as a co-substrate for ring cleavage reactions [15]. It should be reiterated that all exposures that became anaerobic over time initially contained dioxygen that was consumed (<0.1 ppm) by respiration and corrosion reactions. No artificial means of deoxygenation were used in these experiments (e.g. bubbling with N_2).

In the present experiments, all tanks received the same amount of seawater and therefore the same amount of sulfate and chloride as well as the same inoculum. After incubation, all fuel-amended systems also exhibited approximately the same degree of corrosion, even though different patterns of chemical partitioning and fuel constituent biodegradation were observed. Since there was a fixed amount of sulfate in seawater, sulfide influenced corrosion was approximately equal in all incubations, regardless of fuel. In a closed system dissolved sulfides can be potentially inhibitory to SRB. Corroding CS produces ferrous iron (Fe^{+2}) that could react with dissolved sulfide, precipitate solid iron sulfide, and decrease the available dissolved sulfide in the system. Decrease in the concentration of inhibitory dissolved sulfide could permit more SRB activity, fuel degradation and corrosion. The role of Fe^{+2} was similarly acknowledged by Lee and Characklis [16], who concluded that corrosion could not be initiated by SRB on mild steel in the absence of Fe^{+2}. Upon sulfate depletion, anaerobic metabolism can continue, but the flow of carbon and energy likely shifts to methanogenesis. Hamilton [17] developed the hypothesis that dioxygen was required as the terminal electron acceptor in sulfide influenced corrosion, i.e., sulfides produced by SRB react with CS (in this case) to form a sulfide corrosion product. In the absence of dioxygen, corrosion will slow or cease as surface ions are derivitized. In the presence of oxygen the surface-bound sulfides are oxidized and more surface reactions can take place.

5. Conclusions

Corrosion of CS exposed to petroleum- or bio-based alternative fuels (and blends) and seawater was due to reactions with sulfide. Coastal seawater chemistry influenced corrosion with and without fuel addition. The extent of sulfide production could not be predicted from original seawater sulfate concentrations, but was related to the biodegradability of the fuel. Observations related to fuel biodegradation and CS corrosion in fuel/seawater combinations for petroleum-based fuels were similar to those for bio-based fuels with the same basic chemistry. Identical qualitative R_p^{-1} trends were measured for all fuels and both seawaters and appeared to be related to transient dioxygen. Over the course of the experiments, actual R_p^{-1} values for CS exposed to seawater/fuel mixtures varied with fuel composition. The metabolic fate of the water-soluble fuel components from all fuels was influenced by the presence of dioxygen. The presence of diagnostic catechols confirmed that aerobic microorganisms in the seawater initiated the aerobic metabolism of the parent aromatic hydrocarbons.

Acknowledgments

NRL personnel were funded by Sharon Beermann-Curtin at the Office of Naval Research (ONR Code 332) under award N0001411WX21441. NRL publication NRL/JA/7330-12-1550. The study was also supported by grant N000141010946 from the Office of Naval Research.

References

[1] J. Blin, G. Volle, P. Girard, T. Bridgwater, D. Meier, Biodegradability of biomass pyrolysis oils: comparison to conventional petroleum fuels and alternatives fuels in current use, Fuel 86 (2007) 2679–2686.
[2] E.J. Steen, Y.S. Kang, G. Bokinsky, Z.H. Hu, A. Schirmer, A. McClure, S.B. del Cardayre, J.D. Keasling, Microbial production of fatty-acid-derived fuels and chemicals from plant biomass, Nature 463 (2010) 559-U1B2.
[3] P.T. Pienkos, A. Darzins, The promise and challenges of microalgal-derived biofuels, Biofuels Bioprod. Bioref. 3 (2009) 431–440.
[4] D.R. Shonnard, L. Williams, T.N. Kalnes, Camelina-derived jet fuel and diesel: sustainable advanced biofuels, Environ. Prog. Sustainable 29 (2010) 3B2-392.
[S] H.K. Speidel, R.L. Lightner, I. Ahmed, Biodegradability of new engineered fuels compared to conventional petroleum fuels and alternative fuels in current use, Appl. Biochem. Biotech. 84 (2000) 879–B97.
[6] J.S. Lee, R.I. Ray, B.J. Little, Influence of experimental conditions on the outcome of laboratory investigations using natural coastal seawaters, Corrosion 66 (2010) 15001-1S006.
[7] J.S. Lee, R.I. Ray, E.J. Lemieux, A.U. Falster, B.J. Little, An evaluation of carbon steel corrosion under stagnant seawater conditions, Biofouling 20 (2004) 237–247.
[8] J.S. Lee, R.I. Ray, B.J. Little, E.J. Lemieux, Evaluation of deoxygenation as a corrosion control measure for ballast tanks, Corrosion 61 (2005) 1173–118B.
[9] J.R. Scully, Polarization resistance method for determination of instantaneous corrosion rates, Corrosion 56 (2000) 199–218.
[10] Standard reference test method for making potentiostatic and potentiodynamic anodic polarization measurement, ASTM Standard GS-94, ASTM International, West Conshohocken, PA, 2004, pp. 45–56.
[11] Standard practice for preparing, cleaning, and evaluating corrosion test specimens, ASTM Standard G1-03, ASTM International, West Conshohocken, PA, 2003, pp. 17–2S.
[12] D.F. Aktas, J.S. Lee, B.J. Little, R.I. Ray, I.A. Davidova, C.N. Lyles, J.M. Suflita, Anaerobic metabolism of biodiesel and its impact on metal corrosion, Energy Fuel 24 (2010) 2924–292B.
[13] J.S. Lee, R.I. Ray, B.J. Little, An assessment of alternative diesel fuels: microbiological contamination and corrosion under storage conditions, Biofouling 26 (2010) 623–635.
[14] S. Mallick, J. Chakraborty, T.K. Dutta, Role of oxygenases in guiding diverse metabolic pathways in the bacterial degradation of low-molecular-weight polycyclic aromatic hydrocarbons: a review, Crit. Rev. Microbiol. 37 (2011) 64–90.
[1S] J.B. Broderick, Catechol dioxygenases, Essays Biochem. 34 (1999) 173–1B9.
[16] W.C. Lee, W.G. Characklis, Corrosion of mild steel under anaerobic biofilm, Corrosion 49 (1993) 1B6–199.
[17] W.A. Hamilton, Microbiologically influenced corrosion as a model system for the study of metal microbe interactions: a unifying electron transfer hypothesis, Biofouling 19 (2003) 65–76.
[1B] J.S. Lee, R.I. Ray, B.J. Little, Corrosion-related Consequences of Biodiesel in Contact With Natural Seawater, in: CORROSION/2010, NACE International, San Antonio, TX, 2010.
[19] J.S. Lee, R.I. Ray, B.J. Little, K.E. Duncan, A.L. Oldham, I.A. Davidova, J.M. Suflita, Sulphide production and corrosion in seawaters during exposure to FAME diesel, Biofouling 28 (2012) 465–478.
[20] D.F. Aktas, J.S. Lee, B.J. Little, K.E. Duncan, B.M. Perez-Ibarra, J.M. Suflita, Effects of oxygen on biodegradation of fuels in a corroding environment, Int. Biodeterior. Biodegrad. B1 (2013) 114–126.

Jason S. Lee is a Materials Engineer at the US Naval Research Laboratory, Stennis Space Center. He received his PhD in Materials Science and Engineering from the University of Virginia, USA. His research focuses on improved fundamental understanding of the localized corrosion and electrochemistry of metals and alloys exposed to marine environments.

Richard I. Ray is a Physical Scientist at the US Naval Research Laboratory, Stennis Space Center. He received his BS in Biology from the University of Southern Mississippi, USA. He has focused his career on the development of electron microscopy techniques for imaging the biodegradation and biodeterioration of materials in marine environments.

Brenda J. Little is Senior Scientist for Marine Molecular Processes at the US Naval Research Laboratory, Stennis Space Center. She received her PhD in Chemistry from Tulane University, USA and is a National Association of Corrosion Engineers International Fellow. She uses surface analytical chemistry, electron microscopy and electrochemical techniques to investigate adsorption, biofouling, biodegradation and corrosion in marine environments.

Kathleen E. Duncan is a Research Associate Professor in the Department of Microbiology and Plant Sciences, University of Oklahoma, and a member of the University of Oklahoma Biocorrosion Center. She received her PhD in Biology from the University of Rochester, USA. She uses a variety of molecular techniques to determine the genetic diversity, community composition, and physiological capabilities of hydrocarbon-degrading and corrosive microbial communities.

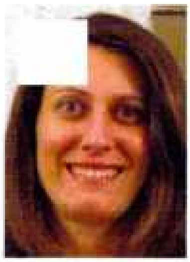

Deniz F. Aktas is a Research Associate in environmental microbiology at the University of Oklahoma. She received her PhD in Chemistry and Biochemistry at the same institution. Her research focuses on anaerobic biodegradation of conventional and alternative fuels and its link to biocorrosion.

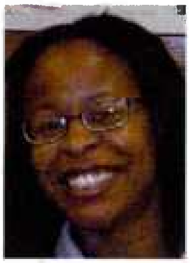

Athenia L. Oldham is a Postdoctoral Researcher in the Department of Microbiology and Plant Biology at the University of Oklahoma. She received her PhD in Cell Biology from the University of Oklahoma Health Sciences Center, and uses metagenomic approaches to understand fuel microbiology.

Irene A. Davidova is a Research Assistant Professor of Botany and Microbiology, University of Oklahoma, Norman, OK, USA. Her interests include environmental microbiology and ecology of anaerobic microorganisms, petroleum microbiology and anaerobic degradation of hydrocarbons.

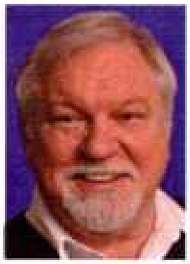

Joseph M. Suflita received his PhD from the Pennsylvania State University and completed his post-doctoral work at the Michigan State University. He is currently a Professor of Microbiology at the University of Oklahoma. His research is focused on the biodegradation of energy-related substances and the relationship of these conversions to metal biocorrosion.